Collective electron description of the conduction mechanism in $M_xFe_{3-x}O_4$, M = Cd,Zn

Hang Nam Ok* and B. J. Evans
Department of Chemistry, University of Michigan, Ann Arbor, Michigan 48109
(Received 8 April 1976)

For $Cd_xFe_{3-x}O_4$ and $Zn_xFe_{3-x}O_4$, the conduction-electron concentration has been varied over a wide range without the introduction of B-site impurities or defects. Analysis of the ^{57}Fe Mössbauer-effect data in terms of the local configurations of Zn^{2+} or Cd^{2+} about a B-site Fe has permitted the influence of the conduction electrons on the electrostatic and magnetic hyperfine interactions to be monitored. For $x \leq 0.3$, the area ratio of the A- and B-site patterns indicates that all B-site ions have nearly identical interactions with the conduction electrons. The isomer shift and magnetic hyperfine field for the local configuration corresponding to Fe_3O_4 tend toward more ferriclike values in a regular fashion as the conduction-electron concentration decreases. Shielding effects at the B-site Fe^{3+} cores by the conduction electrons are manifested in the form of increasing charge and spin transfer from the neighboring ligands with decreasing conduction-electron concentration. Quadrupole splittings are found to be nearly independent of variation in the conduction electron concentration. All of these results, either individually or collectively, require a collective electron description of the conduction mechanism in Fe_3O_4 and no tendency toward localized states at low dopant levels is observed if no defects or impurities are on the B sites.

I. INTRODUCTION

An adequate delineation of the crystal chemical and crystal physical bases for the high electrical conductivity of Fe_3O_4 continues to be elusive. Recent theoretical investigations have reproduced some of the broad systematics of the temperature dependence of the electrical conductivity but the description of the charge carriers is ambiguous and the intuitive crystal chemical insight so necessary to understanding other systems has been lost to some extent in the formalisms of the theoretical models.[1] More importantly, however, is the fact that such models apply only to pure Fe_3O_4 whereas at the present time the electrical properties of "doped" Fe_3O_4 are better understood experimentally than those of pure Fe_3O_4.[2] For example, the B-site impurity-ion concentration at which the conduction mechanism changes from localized hopping to long-range, bandlike itinerancy is known for a number of different dopants.[2,3] However, the behavior of the doped Fe_3O_4 samples involving B-site substitutions is well outside the range of relevance of extant theoretical models. Such models can be modified, however, to account for the properties of "doped" Fe_3O_4 samples in which substitutions of impurity ions is entirely on the A sites. These A-site substituted magnetites have the additional advantage of providing a crystal chemical basis for understanding the variations in electrical properties. Previous ^{57}Fe Mössbauer-effect measurements of Zn-substituted Fe_3O_4 were not subjected to data-analysis techniques that provided answers to current questions[4] as to the localization mechanisms, e.g., pair-localized hopping, and the influence of the magnetic order on the conduction mechanisms, e.g., charge- and spin-density waves; and we have, therefore, conducted a systematic study of Cd- and Zn-substituted Fe_3O_4. In addition, we have sought by means of careful data analysis to clarify the effects of the conduction electrons on the magnetic hyperfine fields, electric quadrupole interaction, and isomer shift at the octahedral site.

Fe_3O_4 (magnetite) has an inverse spinel, AB_2O_4, structure. There are eight AB_2O_4 formula units per face-centered-cubic unit cell. The 32 oxygen ions form a face-centered-cubic close-packed structure. In such a structure there will be three times as many interstices as there are ions forming the structure, e.g., 96. Sixty-four of these interstices are coordinated by four oxygens in a tetrahedral manner and 32 are octahedrally coordinated by oxygen ions. The eight A ions occupy certain selected members of the tetrahedral sites, that is, those at 000 and $\frac{1}{4}\frac{1}{4}\frac{1}{4}$ and six other equivalent positions generated by the primitive fcc translation vectors. Only one-eighth of the tetrahedral sites are occupied. These occupied tetrahedral sites are termed the A sites. Half of the octahedral sites are occupied by the B ions; these occupied sites, located at $\frac{5}{8}\frac{5}{8}\frac{5}{8}$, $\frac{5}{8}\frac{7}{8}\frac{7}{8}$, $\frac{7}{8}\frac{5}{8}\frac{7}{8}$, and $\frac{7}{8}\frac{7}{8}\frac{5}{8}$, plus 12 other equivalent sites generated by the primitive translations of the fcc lattice, are termed the B sites. If the A and B cations are distributed in such a manner that only cations with a +2 oxidation number are present on the A site, then the spinel is said to be a "normal" spinel. If, however, the A-site ions have an oxidation number of +3, the spinel is said to be "inverse"; in this case the B sites are simultaneously occupied by ions with oxidation numbers of +2 and +3. Magnetite

has the cation distribution $(Fe^{3+})[Fe^{2+}, Fe^{3+}]O_4$, where ( ) indicates A-site ions and [ ] indicates B-site ions, and is consequently an inverse spinel, i.e., there are two valence states on the octahedral sites.

In addition to the unusual electrical properties of magnetite, the inverse cation distribution gives rise to strong intersublattice $Fe^{3+}(A)$-O^2-$[Fe^{3+}, Fe^{2+}(B)]$ antiferromagnetic superexchange interactions which lead to the high Néel temperature of the collinear ferrimagnetic spin structure of Fe_3O_4. In the doped magnetites employed in this study, $Zn_xFe_{3-x}O_4$ and $Cd_xFe_{3-x}O_4$, the number of A-O-B superexchange linkages is reduced and, consequently, the Néel temperature and sublattice magnetizations are reduced compared to those of pure Fe_3O_4. The number of B-O-B intrasublattice exchange paths are unaltered by the substitutions, and the effects of changes in the number of conduction electrons can be assessed in an unequivocal fashion.

For the most part, the ^{57}Fe Mössbauer-effect spectra will be sensitive to local parameters of the Fe lattice sites. In magnetite, each B-site ion is surrounded by six nearest-neighbor (NN) oxygen ions at a distance of 2.066 Å, six next-nearest-neighbor (NNN) B-site ions at a distance of 2.969 Å, and six next-next-nearest-neighbor (NNNN) A-site ions at 3.481 Å. Between this NNNN A-site ion shell at 3.481 Å and the NNNNN A-site ion shell, there are four shells of oxygen ions and one shell of B-site ions. It would be adequate, therefore, to take into account only the neighbors up through the six NNNN A-site ions in discussing various local parameters of the B sites. There may be significant long-range interactions that influence the local parameters (especially with respect to the electrical conductivity) but information on these effects is expected to emerge from the data analysis and at any rate, very little can be said *a priori* about such effects.

II. EXPERIMENTAL

The $Zn_xFe_{3-x}O_4$ and $Cd_xFe_{3-x}O_4$ ($x = 0.1, 0.2, 0.3$) samples were prepared by grinding together with acetone appropriate proportions of high-purity (Johnson-Matthey specpure grade) ferric oxide, zinc oxide, cadmium oxide, and iron powder, pressing the resulting mixture into pellets at 6000 kg/cm^2, and firing in low free-volume, evacuated quartz tubes at 1000 and 950°C for zinc- and cadmium-doped magnetites, respectively. The grinding, pressing, and firing operations were repeated at least once. X-ray powder photographs of the samples were taken with a focused Guinier camera using the Cu $K\alpha_1$ line and the diffraction patterns showed the presence of a single spinel phase. The lattice constants were obtained from powder patterns having a silicon internal standard and are tabulated in Table I. It may be noticed that the lattice parameters are nearly unchanged for zinc-doped magnetites while they increase appreciably with increasing cadmium doping level.

TABLE I. Lattice constants of $Zn_xFe_{3-x}O_4$ and $Cd_xFe_{3-x}O_4$.

x	a_0 (10^{-8} cm) $Zn_xFe_{3-x}O_4$	$Cd_xFe_{3-x}O_4$
0.1	8.402 ± 0.008	8.429 ± 0.008
0.2	8.410 ± 0.008	8.469 ± 0.008
0.3	8.413 ± 0.008	8.506 ± 0.008

The Mössbauer absorbers were prepared in the form of disks of 0.5-mm thickness by mixing the samples with transparent lucite powder and applying pressure at 150°C. The absorber density was approximately 10 mg/cm^2 of natural Fe. The Mössbauer spectra were obtained at room temperature with an electromechanical transducer operating in a constant-acceleration mode in conjunction with 1024-channel analyzer. A ^{57}Co source in Rh metal was used for all measurements. The spectrometer was calibrated with a 0.000 64-cm-thick natural iron absorber and the linewidths of all six lines were 0.25 mm/sec.

The spectra were analyzed by means of a least-mean-squares fitting technique. The off-resonant count levels were fitted to a polynomial of second order in the velocity. The lines of the calculated spectrum were assumed to be Lorentzian in shape and no corrections were made for thickness effects. In fitting the spectra the line separations were constrained to be those appropriate to mixed-magnetic hyperfine and electric quadrupole interactions in the limit where $e^2qQ/g_{e_x}\mu H \ll 1$. The relative intensities of the lines were free variables.

III. RESULTS: TREATMENT OF EXPERIMENTAL DATA

The ^{57}Fe Mössbauer spectra of $Zn_xFe_{3-x}O_4$ and $Cd_xFe_{3-x}O_4$, $x = 0.1$, 0.2, and 0.3, are given in Figs. 1 and 2. Assigning the sharper six-line pattern (hereafter termed the A subspectrum) to a well-defined +3 oxidation state of Fe,[4,5] the broader pattern (hereafter termed the B subspectrum) originates from a less-well defined oxidation state of Fe. The broadening of the B pattern is interpreted as being due to a distribution of hyperfine fields at the B site caused principally by a random distribution of NNNN Zn^{2+} or Cd^{2+} ions

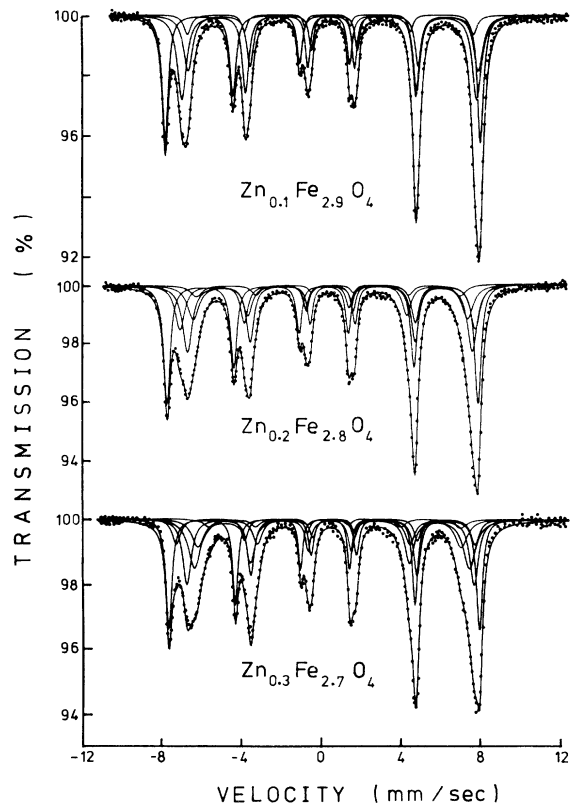

FIG. 1. ^{57}Fe Mössbauer-effect spectra of $Zn_xFe_{3-x}O_4$. The solid lines through the data points are the results of a least-squares fit of several sets of six-line (Lorentzian) patterns to the experimental data. The solid lines above the data points are the individual component lines.

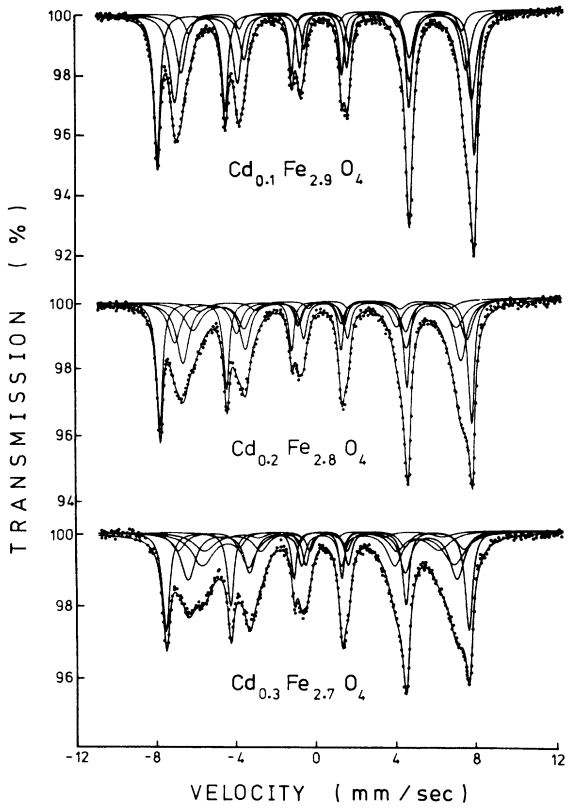

FIG. 2. Mössbauer-effect spectra of $Cd_xFe_{3-x}O_4$. Solid lines and points have the same meaning as in Fig. 1.

at the A sites. This is certainly a reasonable approach to the local configurations and their effects on the magnetic hyperfine interactions; we adopt this description not because it is wholly correct but rather because it is tractable and is the simplest model that will account for the experimental data, e.g., the line shapes of the Mössbauer-effect spectra. Attempts to fit the data to two six-line patterns with Lorentzian line shapes fail for all compositions except $x = 0.0$.

We have therefore fitted the spectra in Figs. 1 and 2 to a model based on a random distribution of Zn and Cd ions on the A sites. In this model B-site Fe ions having different numbers of Zn or Cd ions among their six NNNN A sites have different Mössbauer-effect spectra. The spectra differ primarily in the magnitudes of the magnetic hyperfine fields. The hyperfine fields for the locally different B sites are assumed to obey the following relationship:

$$H_n = H_0(1 - n\Delta H) , \tag{1}$$

where n is the number of Zn or Cd neighbors among the NNNN A sites of the B-site Fe ion that has a hyperfine field H_n. H_0 is the hyperfine field at a B-site Fe ion that has no Zn or Cd A-site neighbors. ΔH is the fractional decrease in the hyperfine field as a result of replacing one A-site Fe^{3+} by Zn^{2+} or Cd^{2+}. The relative intensity of the different B-site spectra is given by

$$P(n,x) = \binom{6}{n} x^n (1-x)^{6-n} , \tag{2}$$

where x is the concentration of Zn or Cd on the A sites. Some typical values of $P(n,x)$ for several values of x are shown in Table II.

TABLE II. Probability $P(n,x)$ of a B site having n diamagnetic ions at the nearest A sites for diamagnetic atomic concentration x at A sites.

n \ x	0.1	0.2	0.3
0	0.531	0.262	0.118
1	0.354	0.393	0.303
2	0.098	0.246	0.324
3	0.015	0.082	0.185
4	0.001	0.015	0.060
5	0.000	0.002	0.010

The spectra were fitted to a mixed-electric quadrupole plus magnetic hyperfine pattern. Only one such pattern was fitted to the A subspectrum; n such patterns were fitted to the B subspectrum subject to the constraint that

$$9.9\times10^{-1}=\sum_{n} P(n,x) \ , \tag{3}$$

in addition to those in Eqs. (1) and (2). The widths and overall intensities of the A and B subspectra were independently varied as free parameters. However, within the two subspectra the following constraints were imposed:

$$I_{s,j,i}=I_{s,j,7-i} \ , \quad \Gamma_{s,j,i}=\Gamma_{s,j,7-i} \ , \tag{4}$$

where $s=A$ or B; $j=1$, when $s=A$, and $j=1,2,\ldots,n$ when $s=B$; and i goes from 1 to 3. The constraints in Eqs. (4) are simply those expected for a thin absorber and an isotropic recoilless fraction f. For the high site symmetry of the B site and the cubic spinel structure f is expected to be isotropic and saturation effects are expected to be small for the sample thicknesses employed.

For each pattern, the electric quadrupole interaction was assumed to have the following general form[6]:

$$\Delta E_Q=\tfrac{1}{8}e^2qQ(3\cos^2\theta-1+\eta\sin^2\theta\cos2\phi) \ , \tag{5}$$

where θ and ϕ are angles in polar coordinates between the magnetic hyperfine-field vector and the principal axes of the electric-field-gradient tensor. This expression holds only when the ratio $e^2qQ/g_{ex}\mu_N H$ is small, which is the case for the $M_xFe_{3-x}O_4$ samples.

The spectra in Figs. 1 and 2 were subjected to a least-mean-squares computer fitting procedure in which $H(A)$, $H_0(B)$, $\Delta H(B)$, $\Delta E_Q(A)$, $\Delta E_Q(B)_n$, $\delta(A)$, $\delta_n(B)$, $I_1(A)$, and $I_{n,1}(B)$ were varied as independent parameters. $\delta(A)$ and $\delta_n(B)$ are, respectively, the isomer shifts for the single A-site pattern and the B-site pattern corresponding to H_n and $P(n,x)$, respectively; $I_1(A)$ and $I_{n,1}(B)$ are the intensities of the first line of the single-A-site pattern and of the B-site pattern corresponding to n, respectively; and the other symbols have their usual meanings. The solid line in Figs. 1 and 2 are the results of the fitting procedure.

The parameters derived from the fitting are given in Table III and IV and in Figs. 3–9.

IV. DISCUSSIONS

The discussion below will be based on the data as illustrated in Figs. 3–9 and Tables I–IV.

A. Area ratios of the A and B subspectrum

As shown in Table III and Fig. 3, the area ratios of the A and B subspectra as fitted in this study

TABLE III. Area ratio of the A and B subspectra for occupancy ratios and average magnetic hyperfine field at B sites for $M_xFe_{3-x}O_4$ samples (M = Zn or Cd).

x	$\left(\frac{A_B}{A_A}\right)_{obs}$	$\frac{[Fe(B)]}{[Fe(A)]}$	$\left(\frac{A_B}{A_A}\right)_{calc}$[a]	$\langle H_B\rangle$
		$Zn_xFe_{3-x}O_4$		
0.1	1.9_1[b]	2.22	2.09	450_1
0.2	2.1_1	2.5	2.35	438_3
0.3	2.7_1	2.85	2.68	431_4
		$Cd_xFe_{3-x}O_4$		
0.1	1.9_1	2.22	2.09	445_3
0.2	2.5_1	2.5	2.35	424_5
0.3	3.1_2	2.85	2.68	395_6

[a] $(A_B/A_A)_{calc}=(f_B/f_A)[Fe(B)/Fe(A)]$, where f_B/f_A is the recoilless-fraction ratio for the B and A sites.

[b] Subscript below each number indicates error in the last digit.

are in good quantitative agreement with that expected if all the Fe ions on the B site contributed to the composite pattern. The area ratio of the B to A subspectra is equal to the following expression when all of the B-site Fe ions contribute to the B subspectra:

$$A_B/A_A=N_Bf_B/N_Af_A=2f_B/(1-x)f_A \ , \tag{6}$$

where N_B and N_A are the number of Fe ions on the B and A sites, respectively, and f_B and f_A are the corresponding recoilless fractions. In computing

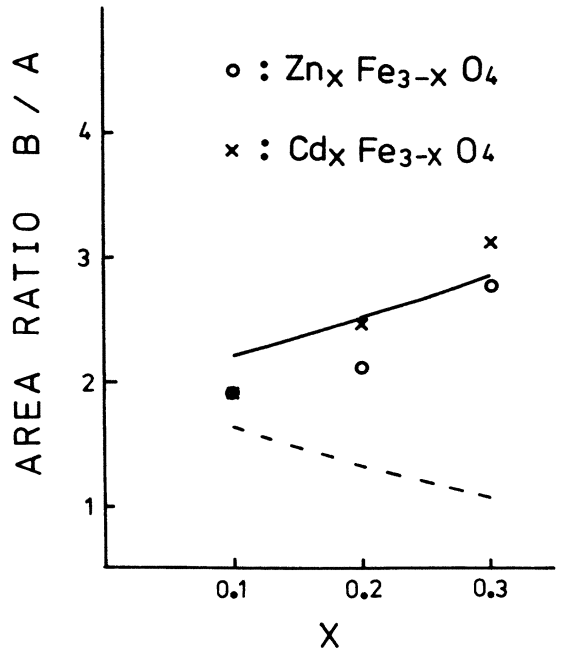

FIG. 3. Area ratio of the B to A subspectra.

$(A_B/A_A)_{calc}$ in Table III, we used the value of 0.94 for f_B/f_A found for pure Fe_3O_4 at 298°K.[7] However, more recent measurements[8] indicate f_B/f_A to be 1.00 ± 0.04 at 298 °K, i.e.,

$$A_B/A_A \cong 2/(1-x) \ . \qquad (6')$$

Equation (5) is plotted as the solid line in Fig. 3. This result is in marked contrast to the area ratios obtained when impurity ions or vacancies are introduced on the B sites.[3,9] In these latter instances, the B/A area ratio is found to be considerably less than the site-occupancy ratios. Interpretations of these data led to the proposal of pairwise hopping in Fe_3O_4 for samples in which the $Fe^{3+}(B)/Fe^{2+}(B)$ ratio differs from 1. For samples in which $Fe^{3+}(B)/Fe^{2+}(B)$ is greater than 1, the presence of isolated Fe^{3+} ions has been invoked to account for the B/A area ratio and the appearance of a third pattern in spectra obtained in an applied magnetic field.[10,11] Based on the results of this study, (localized) pairwise hopping would seem to apply only to magnetite samples that are nonstoichiometric and have vacancies on the B site. Extensive studies[7,10] of nonstoichiometric magnetites in the Fe_3O_4-γ-Fe_2O_3 solid solution series have shown such samples, however, to be inhomogeneous and indicated the presence of an oxidized "γ-Fe_2O_3-like" phase.[7] The area ratios and the appearance of a third pattern attributable to an "Fe^{3+}-like" species in nonstoichiometric magnetites are all consistent with a γ-Fe_2O_3 or γ-Fe_2O_3-like phase being present.[11] Even though the effects of B-site dopants are substantially greater than those for nonmagnetic A-site dopants, the effect of Ni^{2+} at low dopant levels, for example, on the conduction process as evidenced by the linewidths of the ^{57}Fe Mössbauer-effect spectra is minor, and isolated $Fe^{3+}(B)$, as expected on the basis of the pairwise hopping model, do not exist in $Ni_xFe_{3-x}O_4$ up to $x = 0.4$.[3]

The broken line in Fig. 3 shows $2(1-x)/(1+x)$, which would be the area ratio of the B to A subspectra assuming that the pair-localized electron hopping model is valid and the "isolated" $Fe^{3+}(B)$ ions are included in the ferric A subspectrum.[9] The area ratios of A and B subspectra in the Zn- and Cd-doped magnetites determined in this study are strong evidence for the participation of all B-site Fe ions in the processes giving rise to the high electrical conductivity.

A rigorous treatment of a pair-localized model would lead to a more complicated expression than $2(1-x)/(1+x)$ for the B-to-A area ratio. Such a treatment would involve calculating the probability $P(n,x)$ that a given B-site Fe^{3+} ion would have no Fe^{2+} B-site neighbors. However, such a calculation would not be applicable to pure Fe_3O_4 even though the probability of isolated Fe^{3+} ions is 2%; in fact there are no isolated Fe^{3+} ions in pure Fe_3O_4. In addition, the existence of isolated Fe^{3+} ions in materials in which only Fe ions are located on the B sites requires the absence of Fe^{2+} ions among the B-site neighbors of a given $Fe^{3+}(B)$ as a necessary condition; but this condition is not sufficient. For example, an "isolated" Fe^{3+} ion is shown in configuration 1:

Configuration 1:

$$Fe^{3+}(B)\text{-}O^{2-}\text{-}[Fe^{3+}(B)]_6 \ .$$

This configuration, however, does not establish that the $Fe^{3+}(B)$ ion is isolated, for if an Fe^{2+} ion is a next nearest neighbor to this ion as shown in configuration 1′ electron delocalization can take place as shown in configuration 1″.

Configuration 1′:

$$Fe^{3+}(B)\text{-}O^{2-}\text{-}[Fe^{3+}(B)]_6\text{-}O^{2-}\text{-}Fe^{2+}(B).$$

Configuration 1″:

$$Fe^{2+}(B)\text{-}O^{2}\text{-}[Fe^{3+}(B)]_6\text{-}O^{2-}\text{-}Fe^{3+}(B).$$

Configurations 1′ and 1″ are identical to each other. There must also be no B-site Fe^{2+} ions that are next nearest neighbors to a given $Fe^{3+}(B)$ if this ion is to be isolated, as shown in configuration 2.

Configuration 2 (isolated Fe^{3+} ion):

$$Fe^{3+}(B)\text{-}O^{2-}\text{-}[Fe^{3+}(B)]_6\text{-}O^{2-}\text{-}Fe^{3+}(B).$$

The weak influence of the dopants on the hyperfine parameters and the retention of a collective electron state for the conduction electrons even though $[Fe^{3+}(B)]/[Fe^{2+}(B)] \neq 1$ demonstrate that Fe_3O_4 is not as close to the collective-electron $\leftrightarrow$ localized-electron phase boundary as previously believed[12]; Fe_3O_4 seems to be well within the phase field for collective electron behavior. Previous conundri[12] arising from the belief that the electronic structure of Fe_3O_4 is close to the collective electron-localized electron phase boundary are removed by the above considerations.

B. Isomer shifts

As shown in Fig. 4, the isomer-shift difference between the B-site Fe ions with no Zn neighbors and the A-site ferric ions decreases as the number of conduction electrons decreases. In other words, the $n = 0$ B-site ions become more ferric-like. Assuming that the conduction electrons interact more or less equally with all of the B-site ions as in the case of a band description of the itinerant electrons, the isomer-shift difference between the A and B sites will be approximately proportional to the number of conduction electrons;

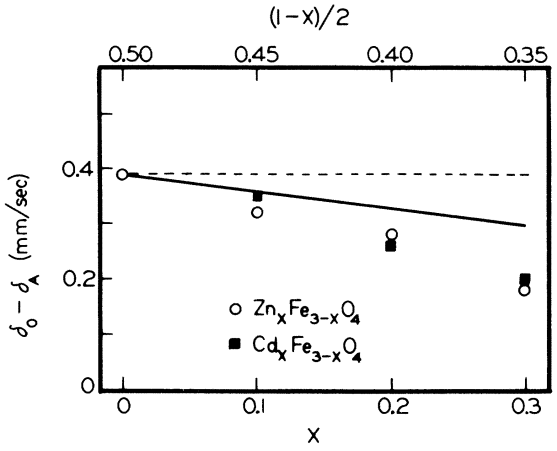

FIG. 4. Isomer-shift difference between B-site iron ions with $n=0$ and A-site ferric ions as a function of the diamagnetic ion concentration x or the number of conduction electrons per B site, $(1-x)/2$.

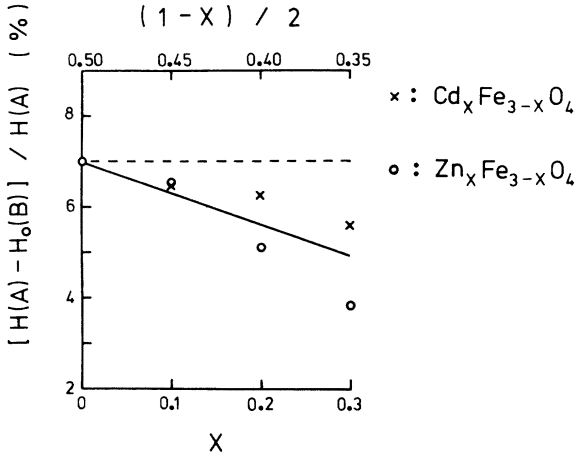

FIG. 5. Ratio of the difference $H(A)-H_0(B)$ to $H(A)$ as a function of x or the number of conduction electrons per B site, $(1-x)/2$.

that is to say,

$$\delta_0(x)-\delta_A(x)=[\delta_0(0)-\delta_A(0)-C][0.5(1-x)/0.5]+C\ , \tag{7}$$

where $\delta_A(x)$ and $\delta_0(x)$ are the isomer shifts of the A-site ferric ions and B-site ions with $n=0$, respectively, when the dopant concentration on the A site is x. C is the value of $\delta_0(x)-\delta_A(x)$ when $x=1$, i.e., Fe^{3+} ions are on both A and B sites. In this case the difference is due to covalence and is approximately 0.1 mm sec^{-1}. Equation (7) is drawn as the solid line in Fig. 4.

These considerations would apply only to the A-site Fe ions and the B-site ions for which $n=0$, since the isomer shifts for B-site ions with $n\neq 0$ would change in response to differences in local crystal chemistry occasioned by the substitution of a divalent ion for a trivalent ion among their A-site neighbors, and by the different Fe-O internuclear separation when Zn^{2+} is substituted for $Fe^{3+}(A)$.

The broken line in Fig. 4 shows what would be expected on the basis of the pair-localized hopping model, in which the average charge state within Fe^{2+}-Fe^{3+} pairs would $Fe^{2.5+}$ and independent of x. This would result in constant isomer shift which is in disagreement with the data.

C. Magnetic hyperfine fields

1. *Magnetic hyperfine field at B site with no Zn or Cd neighbors*

The ratio of the difference $H(A)-H_0(B)$ to $H(A)$ is plotted in Fig. 5 as a function of x or the number of conduction electrons per B site. Since the spin direction of the conduction electrons is opposite to that of the Fe^{3+} cores, a decrease in the conduction-electron concentration tends to increase the total moment of the B sublattice. If T/T_N were constant as x increases, the magnitude of $H_0(B)$ would be expected to increase; this result is expected irrespective of whether the conduction-electron–4s or conduction-electron–3d interaction is dominant. However, since the presence of A-site Zn^{2+} lowers the Néel temperature, the magnetization of the B (and A) sites decreases with increasing x and the effect of the decrease in overall magnetization on $H_0(B)$ must be taken into account. This can be done in the following manner: For small x values, the reduced magnetization of the A and B sites will be approximately equal; and changes in $H_0(B)$ over and above those resulting from the decrease in bulk magnetization can be assessed by using $H(A)$ as the reference field at each x value.

Therefore, for a band description of the conduction electrons in $M_xFe_{3-x}O_4$ the following relationship between hyperfine fields would hold for small x values:

$$[H_A(x)-H_0(x)]/H_A(x)=\{[H_A(0)-H_0(0)]/H_A(0)\}(1-x), \tag{8}$$

where $(1-x)/2$ is the conduction-electron concentration on the B site and $H_A(x)$ and $H_0(x)$ are the magnetic hyperfine fields at the A sites and the B site with $n=0$, respectively. Equation (8) is drawn in Fig. 5 as the solid line, which is in reasonable conformity with the experimental points. The agreement is quite good at low x values, where Eq. (8) is expected to be a good approximation. Actually, if a B-site hyperfine field for $n=0$, e.g., $H_0(y)$, in an insulating ferrite were available, where

y is the concentration of Zn that gives the same bulk magnetization as the concentration x in Fe_3O_4, it could be substituted for $H_A(x)$ in Eq. (8). Then, Eq. (8) would be a good approximation over a much larger range of x values and would at least satisfy the boundary conditions at $x = 0$ and $x = 1$. In its present form, it satisfies the boundary conditions only at $x = 0$. The needed values of $H_0(y)$ for $n = 0$ are not currently available.

For a pair-localized hopping model, the decrease in the conduction-electron concentration would result in a decreasing number of Fe^{2+}-Fe^{3+} pairs but the conduction-electron–ion-core Coulomb and magnetic exchange interactions would be constant within pairs. In this case, $[H_A(x) - H_0(x)]/H_A(x)$ would be constant and independent of x in disagreement with the data in Fig. 5. Furthermore, even though there may be a strong intersublattice Zn^{2+} and Fe^{3+} ordering (that is, a tendency for Zn^{2+} to be among the A-site neighbors of an Fe^{3+} ion as opposed to an Fe^{2+} or $Fe^{2+} \rightarrow Fe^{3+}$ averaged species), the $(n = 0)$-site ions are the ones most likely to be involved in any collective electron interactions. Our consideration of this particular type of B-site ion provides strong evidence for a band description of the conduction electrons in these doped samples.

2. *Change in magnetic hyperfine field as function of Zn or Cd neighbors*

In Fig. 6, the fractional changes of the magnetic hyperfine field are plotted as a function of x; the absolute values of ΔH[cf. Eq. (1)] are listed in Table IV. Both the absolute and fractional values increase with decreasing conduction-electron concentration. No simple interpretation can be given to this behavior since several effects[13] contribute

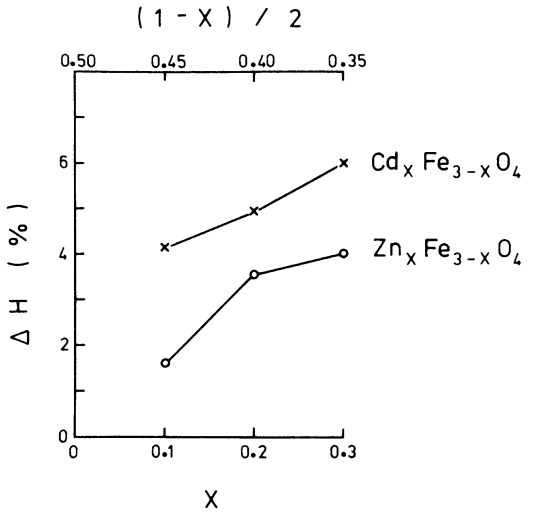

FIG. 6. Fractional change of the magnetic hyperfine field at B site per diamagnetic Zn or Cd ion as a function of x and conduction-electron concentration.

to the magnetic hyperfine field. For example, ΔH would be expected to increase as x increases due simply to the decreased bulk magnetization, especially if T/T_N approaches a value near the "knee" of the magnetization curve. However, the fractional value of ΔH is larger than that in $Zn_xNi_{1-x}Fe_{2-x}O_4$; $\Delta H/H_0$ does not exceed 2% in the nickel-zinc ferrites[14] but is 3 to 5% for the doped magnetites being considered here. The substantially larger values of $\Delta H/H_0$ for $M_xFe_{3-x}O_4$ can be understood qualitatively in terms of the influence of the conduction-electron concentration on the super-transferred hyperfine fields and magnetic exchange interactions.

The conduction electrons decrease the hyperfine field at the B-site Fe ions by two mechanisms, at

TABLE IV. Some of the results obtained in least-squares fits of 4–6 sets of six line patterns to the Mössbauer spectra of $Zn_xFe_{3-x}O_4$ and $Cd_xFe_{3-x}O_4$ at room temperature.

x	H_A[a] (kOe)	H_0[a] (kOe)	$H_0\Delta H$ (kOe)	$S_0 - S_A$ (mm/sec)	$(\Delta E_Q)_0$ (mm/sec)	$(\Delta E_Q)_A$ (mm/sec)
			$Zn_xFe_{3-x}O_4$			
0.1	486_1[b]	454_1	7.2_1	0.32_1	-0.04_1	-0.039_5
0.2	481_1	457_1	16.3_6	0.28_1	-0.06_1	-0.035_5
0.3	481_1	463_1	18.4_5	0.18_1	-0.13_2	-0.028_5
			$Cd_xFe_{3-x}O_4$			
0.1	487_1	456_1	18.9_6	0.35_1	-0.02_1	-0.039_5
0.2	481_1	451_1	22_1	0.26_1	-0.02_1	-0.034_5
0.3	468_1	442_2	27_1	0.20_4	-0.03_3	-0.028_5

[a] Subscripts A and 0 indicate values at A sites and B sites with no diamagnetic neighbor atom, respectively.

[b] Subscript below each number indicates estimated error in the last digit.

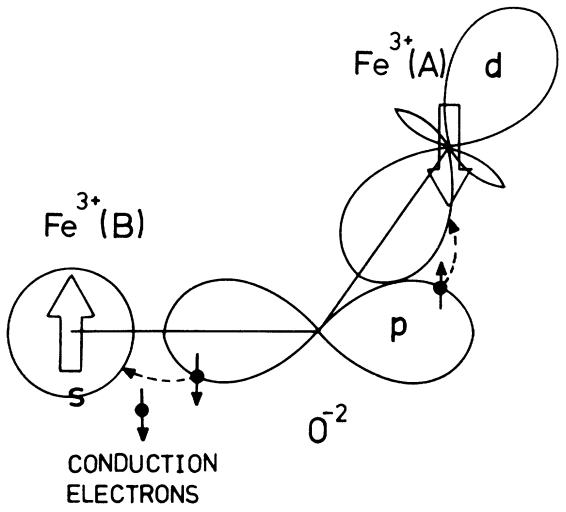

FIG. 7. Schematic diagram of the effects of conduction electrons on the supertransferred hyperfine field. The large arrows represent the Fe^{3+}core spins at the A and B sites.

least. First of all, there is substantial mixing of the conduction electrons with the local d wave functions. The large isomer shift and substantially reduced hyperfine field virtually require this. Second, the conduction electrons reduce the hyperfine field by screening the Fe^{3+} ion cores and reducing the charge and spin transfer from the oxygen ions to the 4s orbital of the B-site ions, as shown in Fig. 7. The screening by the conduction electrons has the effect, therefore, of diminishing the supertransferred hyperfine interactions. There are other overlap and covalence mechanisms for the supertransferred interactions but the covalent transfer into the 4s orbital is the dominant one for spinel oxides.[14,15] Therefore, a decrease in the conduction-electron concentration would cause an increase in the B-site hyperfine field based on the first mechanism. Indeed, H_0 does increase for the Zn-doped samples, More precisely, however, the fields are not expected to increase if the decrease in the Néel temperature is also substantial, as in the case of the Cd-doped samples. In this instance, a slowly decreasing or constant (for small x) magnetic hyperfine field is expected. This is the observed behavior for the Cd-doped samples.

The situation is somewhat more complicated for B sites that have Cd and Zn A-site neighbors. The weakening of the superexchange interactions by the Zn ions and consequent reduction in the local magnetization is expected to offset any tendency for the decrease in the conduction-electron concentration to increase the magnetic hyperfine field. Thus, we expect the magnetic hyperfine field at B sites having Zn and Cd A-site neighbors to decrease with increasing x. The unique aspect of the results for substituted magnetites is that the decrease is greater than that for insulating ferrites. As we have shown, the conduction electrons have very similar interactions with the B-site Fe^{3+} cores irrespective of their A-site environments. Therefore, for the B-site configurations with Zn and Cd A-site neighbors, not only is there a decrease in the magnetic hyperfine field due to the decreased exchange interactions but the interaction of the ion cores with the conduction electrons is also causing a decrease in the field. Thus, the net decrease will be substantially greater than that in insulating ferrites. A further decrease arises because even though the dominant effect of the conduction electrons is to screen the B sites, they also augment the magnitude of the hyperfine field through their interaction with the 4s orbital, as depicted in Fig. 7. This effect is negligible for small changes in the conduction-electron concentration, as in the case of $Zn_xFe_{3-x}O_4$. However, for $Cd_xFe_{3-x}O_4$ the decrease in the conduction-electron concentration with increasing x is substantial, owing to the larger increase in the volume, and is six times as large as that for $Zn_xFe_{3-x}O_4$. Thus the magnitude of ΔH is substantially larger for $Cd_xFe_{3-x}O_4$ than for $Zn_xFe_{3-x}O_4$. The larger decrease in the strengths of the magnetic exchange interactions as a result of the volume increase also serves to make ΔH larger for $Cd_xFe_{3-x}O_4$.

D. Electric quadrupole interaction

Figure 8 shows quadrupole splittings at B sites as functions of n (the number of diamagnetic neigh-

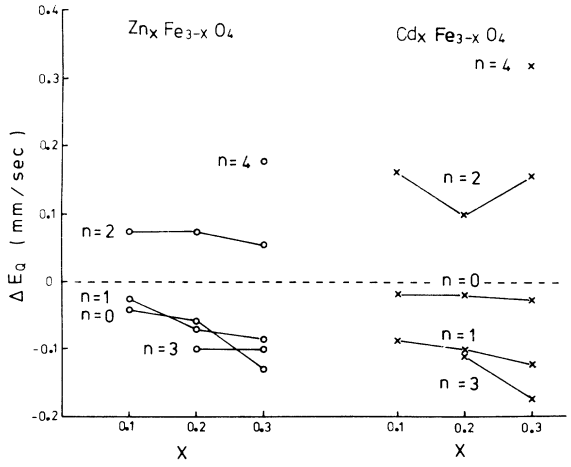

FIG. 8. Quadrupole splitting at B site as functions of concentration of diamagnetic ions and the number of diamagnetic neighbors at A sites.

bors) and x. There are two noticeable points; one is that all $(\Delta E_Q)_n$ lines for fixed n values are roughly parallel to the x axis and the other one is that the ΔE_Q varies somewhat erratically as n changes. The first behavior can be explained by invariancy of local symmetries at B sites with respect to variation of the number of conduction electrons. To get a clear picture of the second behavior the average values of $(\Delta E_Q)_n$ taken with respect to x are shown in Fig. 9. $\langle \Delta E_Q \rangle$ change signs as each diamagnetic ion is added. However, the absolute value of $\langle \Delta E_Q \rangle$ monotonically increases as n increases, which can be understood in terms of increasing deviation of local symmetry from the cubic symmetry. The sign change may originate from the angular factor of Eq. (4). According to the neutron diffraction measurements[16] the spin directions of the magnetic ions in magnetite are along one of the cubic axes, while the trigonal axis at a B site is along one of the [111] directions. Thus, the principal axis of the maximum electric field gradient would be close to this [111] direction even for Zn- or Cd-doped magnetites because the nearest A sites of a B site are actually the next, next nearest neighbors, and the conduction electrons prevailing among the intervening B sites can screen the diamagnetic divalent ions. Therefore, $\cos\theta \simeq 1/\sqrt{3}$. Now as diamagnetic ions replace Fe^{3+} ions at the nearest A sites, the $3\cos^2\theta - 1$ term may be positive or negative depending on whether $\cos\theta$ becomes greater or smaller than $1/\sqrt{3}$. The sign of the $\eta \sin^2\theta \cos 2\phi$ term also can change drastically depending on whether ϕ becomes greater or smaller than 45°.

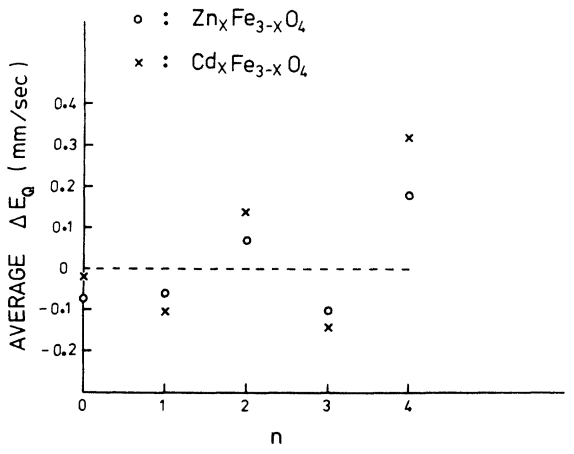

FIG. 9. Average quadrupole splittings at B sites as a function of the number of diamagnetic A-site neighbors.

V. CONCLUSIONS

Through careful but straightforward analysis of the 298°K ^{57}Fe Mössbauer-effect spectra of $Cd_xFe_{3-x}O_4$ and $Zn_xFe_{3-x}O_4$ for $0 < x < 0.3$, conclusive evidence is obtained for the validity of a band description of the conduction electrons in pure and doped Fe_3O_4 (low doping levels) when no foreign ions are present on the B sites. These results indicate that while the electronic structure of Fe_3O_4 might be close to that of the collective electron-localized electron phase boundary, the conduction mechanism has a strong bandlike character and is little affected by slight changes in the conduction-electron concentration. The data analysis technique which permitted us to focus our attention on the local B-site configuration that resembles that in pure Fe_3O_4 has been crucial to the success of this study. Little concern is raised, however, over the model dependence of our results since the data-analysis technique has been applied successfully to a broad class of inverse spinel ferrites.

More specifically, the following has been shown:

(i) The ratio of the total area of the B-site subspectrum to that of the A-site subspectrum was the same as the ratio of Fe ions on these two sites. This result demonstrates that all of the B-site ions are involved in the conduction even when the number of conduction electrons per B site is quite different from 0.5. No evidence was found for the existence of isolated Fe^{3+} (or Fe^{2+}) for values as high as 0.3.

(ii) The magnitude of the decrease in the B-site hyperfine field brought on by the presence of Zn^{2+} ions among its A-site neighbors increases as the conduction-electron concentration decreases. This result is understandable in terms of the magnetic exchange interaction, supertransferred hyperfine fields, and the shielding of the $Fe^{3+}(B)$ cores by the conduction electrons. This interpretation is confirmed by the larger effect occasioned by Cd substitution, for which case the conduction-electron concentration and magnetic exchange interactions decrease more rapidly with x than for $Zn_xFe_{3-x}O_4$. A collective electron description of the conduction electrons is virtually demanded by these results.

(iii) The isomer shift at the B-site Fe ions that have no A-site Zn^{2+}neighbors shows a regular shift toward a more ferriclike charge state as the conduction-electron concentration decreases. Since these Fe ions are the ones most likely to be engaged in electron delocalization processes, the results are consistent with those expected on the basis of a band model in which a decrease in the conduction-electron concentration would be mani-

fest at all of the B sites. Unlike the situation for the hyperfine fields, the effects of Cd doping are not expected to lead to a more ferriclike charge state than Zn doping since the Fe–O–B-site bonds become more covalent with increasing x for Cd despite the increase in lattice constant. This increase in covalence causes a decrease in the isomer shift that partially offsets the increase expected on the basis of the decrease in the conduction-electron concentration. The net result is that the isomer-shift dependence on electron concentration is nearly the same for Cd and Zn doping.

(iv) The electric quadrupole interaction is rather insensitive to decreases in the conduction-electron concentration and the asymmetry introduced in the environment of a B site by Zn and Cd substitution. The conduction electrons are expected to have only a small direct influence on the electric field gradient, but the small influence of the Zn and Cd ions is unexpected. This could be explained by the conduction-electron screening of the B-site ions from charge asymmetries among neighboring sites and would be consistent with a band model for the conduction electrons. It would be indiscreet, however, to attach any great significance to this interpretation of the electric field gradient.

ACKNOWLEDGMENTS

Support of this study by the National Science Foundation, under Grant GH-41419, and the Division of Research Development and Administration of the University of Michigan is gratefully acknowledged.

---

*On leave from Department of Physics, Yonsei University, Seoul, Korea.

[1]J. R. Cullen and E. R. Callen, Phys. Rev. B 7, 397 (1973); B. Lorentz, Phys. Status Solidi B 69, 451 (1975).

[2]J. Bunget, C. Nistor, and M. Rosenberg, J. Phys. (Paris) 32, C1-274 (1971); C. Constantin and M. Rosenberg, AIP Conf. Proc. 10, 1389 (1972).

[3]J. W. Linnett and M. M. Rahman, J. Phys. Chem. Solids 33, 1465 (1972).

[4]D. C. Dobson, J. W. Linnet, and M. M. Rahman, J. Phys. Chem. Solids 32, 2727 (1970).

[5]B. J. Evans, AIP Conf. Proc. 10, 1398 (1972).

[6]H. N. Ok and J. G. Mullen, Phys. Rev. 168, 563 (1968).

[7]H. P. Weber, Ph.D. thesis (University of Chicago, 1971) (unpublished).

[8]M. Robbins, G. K. Wertheim, R. C. Sherwood, and D. N. E. Buchanan, J. Phys. Chem. Solids 32, 717 (1971).

[9]J. M. Daniels and A. Rosencwaig, J. Phys. Chem. Solids 30, 1561 (1969).

[10]H. Annersten and S. Hafner, Z. Kristallogr. 137, 321 (1973).

[11]J. M. D. Coey, A. H. Morrish, and G. A. Sawatzky, J. Phys. (Paris) 32, C-271 (1971).

[12]J. B. Goodenough, Solid State Chem. 5, 145 (1972).

[13]F. van der Woude and G. A. Sawatzky, Phys. Rev. B 4, 3159 (1971); C. Boekema, F. van der Woude, and G. A. Sawatzky, Int. J. Mag. 3, 341 (1972).

[14]L. K. Leung, B. J. Evans, and A. H. Morrish, Phys. Rev. B 8, 29 (1973).

[15]M. A. Butler, E. Eibschütz, and L. G. Van Uitert, Solid State Commun. 12, 499 (1973).

[16]C. G. Shull, E. O. Wollan, and W. C. Koehler, Phys. Rev. 84, 912 (1951); W. C. Hamilton, Phys. Rev. 110, 1050 (1958).